

## New high accuracy measurement of the $^{17}\text{O}(p,\alpha)^{14}\text{N}$ reaction rate at astrophysical temperatures

M. L. Sergi,<sup>1,\*</sup> C. Spitaleri,<sup>1,†</sup> M. La Cognata,<sup>1</sup> A. Coc,<sup>2</sup> A. Mukhamedzhanov,<sup>3</sup> S. V. Burjan,<sup>4</sup> S. Cherubini,<sup>1</sup> V. Crucillá,<sup>1</sup> M. Gulino,<sup>1</sup> F. Hammache,<sup>5</sup> Z. Hons,<sup>4</sup> B. Irgaziev,<sup>6</sup> G. G. Kiss,<sup>1</sup> V. Kroha,<sup>4</sup> L. Lamia,<sup>1,\*</sup> R. G. Pizzone,<sup>1</sup> S. M. R. Puglia,<sup>1</sup> G. G. Rapisarda,<sup>1</sup> S. Romano,<sup>1</sup> N. de Séréville,<sup>5</sup> E. Somorjai,<sup>7</sup> S. Tudisco,<sup>1</sup> and A. Tumino<sup>1,‡</sup>

<sup>1</sup>*Dipartimento di Metodologie Fisiche e Chimiche per l'Ingegneria, Università di Catania, and INFN-Laboratori Nazionali del Sud, Catania, Italy*

<sup>2</sup>*Centre de Spectrométrie Nucléaire et de Spectrométrie de Masse, UMR 8609, CNRS/IN2P3 and Université Paris Sud 11, Bâtiment 104, F-91405 Orsay Campus, France*

<sup>3</sup>*Cyclotron Institute, Texas A&M University College Station, Texas, USA*

<sup>4</sup>*Nuclear Physics Institute of ASCR Rez near Prague, Czech Republic*

<sup>5</sup>*Institut de Physique Nucléaire, UMR-8608, CNRS/IN2P3 and Université Paris-Sud XI, F-91406 Orsay, France*

<sup>6</sup>*GIK Institute of Engineering Sciences and Technology, Topi District, Swabi NWFP, Pakistan*

<sup>7</sup>*ATOMKI, Debrecen, Hungary*

(Received 17 February 2010; published 8 September 2010)

The  $^{17}\text{O}(p,\alpha)^{14}\text{N}$  reaction is of fundamental relevance in several astrophysical scenarios, such as novae, asymptotic giant branch nucleosynthesis, and  $\gamma$ -ray astronomy. We report on the indirect measurement of the  $^{17}\text{O}(p,\alpha)^{14}\text{N}$  reaction bare-nucleus cross section in the low-energy region. In particular, the two resonances at  $E_R^{c.m.} = 65$  keV and  $E_R^{c.m.} = 183$  keV, which dominate the reaction rate inside the Gamow window, have been observed, and the strength of the 65 keV resonance has been deduced. The reaction rate determination and the comparison with the results of the previous measurements are also discussed.

DOI: [10.1103/PhysRevC.82.032801](https://doi.org/10.1103/PhysRevC.82.032801)

PACS number(s): 26.20.-f, 26.30.-k, 24.30.-v, 24.50.+g

The  $^{17}\text{O}$  abundance plays a key role both in novae nucleosynthesis and in  $\gamma$ -ray astronomy. This rare isotope is processed in the CNO cycle, and it is important for the subsequent formation of the short-lived  $^{18}\text{F}$  radioisotope, of special interest in novae observations in the  $\gamma$ -ray wavelengths. In fact, it decays appreciably when the envelope begins to be transparent enough to let  $\gamma$  rays be transported through the whole envelope and emitted into space. Thus, the amount of emitted radiation strongly depends on the  $^{18}\text{F}$  supply in the nova envelope [1,2].  $^{17}\text{O}$  intervenes in the  $^{18}\text{F}$  production through the reaction chain  $^{16}\text{O}(p,\gamma)^{17}\text{F}(\beta^+)^{17}\text{O}(p,\gamma)^{18}\text{F}$ . However, the  $^{18}\text{F}$  production yield is also affected by the  $^{17}\text{O}(p,\alpha)^{14}\text{N}$  reaction channel that removes  $^{17}\text{O}$  nuclei from  $^{18}\text{F}$  production path and competes with the  $(p,\gamma)$  reaction at all temperatures relevant to novae ( $T_9 = T/10^9$  K = 0.01–0.4). Moreover, the  $^{17}\text{O}(p,\alpha)^{14}\text{N}$  reaction influences the  $^{17}\text{O}/^{16}\text{O}$  isotopic ratio, which plays a crucial role to constrain extra-mixing processes in AGB stars [3]. This ratio is known with very high accuracy since it is measured in pre-solar grains. Several oxide grains, showing a low value of  $^{18}\text{O}/^{16}\text{O}$  and a  $^{17}\text{O}/^{16}\text{O}$  ratio much larger than the solar one, are formed in low-mass asymptotic giant branch (AGB) stars ( $<2.5M_\odot$ ) [4]. Since  $^{16}\text{O}$  is the most abundant isotope and its abundance is essentially unchanged throughout stellar evolution, and because  $^{18}\text{O}$  and  $^{17}\text{O}$  are not affected by He-burning instabilities, the “anomalies” in the oxygen isotopic ratios found in oxide grains are considered the

signature of deep mixing phenomena in AGB stars [3,5]. In the transported material, proton capture nucleosynthesis can take place at relatively low temperatures ( $T_9 < 0.04$ ). In particular, the  $^{17}\text{O}$  abundance results from the competition between the  $^{16}\text{O}(p,\gamma)^{17}\text{F}(\beta^+)^{17}\text{O}$  production channel and the  $^{17}\text{O}(p,\alpha)^{14}\text{N}$  destruction rate. In this framework, the  $^{17}\text{O}(p,\alpha)^{14}\text{N}$  reaction influences the  $^{17}\text{O}$  yield and thus a revised reaction rate may help to constrain mixing models.

Because of its key importance to astrophysics, the cross section of the  $^{17}\text{O}(p,\alpha)^{14}\text{N}$  reaction has been the subject of several experimental investigations [6–15], but its knowledge is presently insufficient at low temperatures. The relevant stellar temperatures for the  $^{17}\text{O}$  nucleosynthesis are in the ranges  $T_9 = 0.01$ –0.1 for red giants, AGB, and massive stars, and  $T_9 = 0.01$ –0.4 for classical nova explosions [2]. Thus, the  $^{17}\text{O}(p,\alpha)^{14}\text{N}$  and  $^{17}\text{O}(p,\gamma)^{18}\text{F}$  reaction cross sections have to be precisely known in the center-of-mass energy range  $E_{c.m.} = 0.017$ –0.370 MeV.

In this energy range, the  $^{17}\text{O}(p,\alpha)^{14}\text{N}$  reaction cross section is dominated by two resonances: one at about 65 keV above the  $^{18}\text{F}$  proton threshold, corresponding to the  $E_x = 5.673$  MeV level in  $^{18}\text{F}$ , and one at 183 keV ( $E_x = 5.786$  MeV). In the last few years, several measurements [11,13,14] of the  $E_R^{c.m.} = 183$  keV resonance both in the  $(p,\gamma)$  and  $(p,\alpha)$  channels have drastically reduced the uncertainties on both  $^{17}\text{O}(p,\alpha)^{14}\text{N}$  and  $^{17}\text{O}(p,\gamma)^{18}\text{F}$  rates in the context of explosive H burning, whereas only one direct measurement [10] of the  $E_R^{c.m.} = 65$  keV resonance was performed in the  $(p,\alpha)$  channel. In fact, direct measurements of resonance strengths at very low energies, as in the case of the 65 keV resonance, are very difficult because of the Coulomb barrier suppressing the cross section down to a few nb. In particular, in the direct measurement of Ref. [10], a  $\Gamma_p = 22 \pm 3_{\text{stat}} \pm 2_{\text{target-1 beam}}^{+2}$  neV

\*Present address: EC-JRC-Institute for Reference Materials and Measurements (IRMM), Retieseweg 111, B-2440 Geel, Belgium.

†Spitaleri@Ins.infn.it

‡Present address: Università Kore di Enna, Enna, Italy.

proton width of the 65 keV resonance was found, which is the smallest measured proton-capture width. However, the screening of the nuclear Coulomb field by atomic electrons was not taken into account in Ref. [10]. Indeed, at these energies, atomic electron clouds can shield the nuclear charges of the interacting nuclei and might determine an enhancement of the cross section larger than 15% [16] for the  $^{17}\text{O} + p$  system that cannot be neglected for astrophysical purposes.

In this paper, we report on the indirect measurement of the  $^{17}\text{O}(p,\alpha)^{14}\text{N}$  reaction at energies below 300 keV. Both the 65 and 183 keV resonances were observed and the  $^{17}\text{O}(p,\alpha)^{14}\text{N}$  reaction rate deduced with improved accuracy in the temperature range below  $T_9 = 0.2$  and well established, for the first time, below  $T_9 = 0.1$ . To study the  $^{17}\text{O}(p,\alpha)^{14}\text{N}$  reaction at such low energies, we used the trojan horse method (THM) [17–19]. This is an indirect technique that, by selecting the quasifree (QF) contribution to a suitable three-body reaction  $A + a(x + s) \rightarrow c + C + s$  performed at energies well above the Coulomb barrier, leads to the extraction of the cross section of the binary reaction  $A + x \rightarrow c + C$  at astrophysical energies, unhindered by Coulomb suppression [18–28].

In particular, the present study of the  $^{17}\text{O}(p,\alpha)^{14}\text{N}$  reaction was performed in the energy window relevant to astrophysics by selecting the QF contribution to the  $^2\text{H}(^{17}\text{O},^{14}\text{N}\alpha)n$  reaction. The deuteron was used as the “trojan horse nucleus” because of its  $p$ - $n$  structure; the proton is brought into the nuclear field of  $^{17}\text{O}$ , while the neutron acts like a spectator to the binary quasifree reaction.

The experiment was performed at the Laboratori Nazionali del Sud in Catania, Italy. The SMP tandem Van de Graaff accelerator provided a 41 MeV  $^{17}\text{O}$  beam impinging on deuterated polyethylene targets ( $\text{CD}_2$ ),  $\sim 150 \mu\text{g}/\text{cm}^2$  thick, perpendicular to the beam axis. The detection setup consisted of six silicon position sensitive detectors (PSDs). The forward one was centered at  $7.6^\circ$ , covering a  $\Delta\theta = 5^\circ$  angular region and optimized for  $^{14}\text{N}$  detection; the second and the third ones, optimized for the  $\alpha$ -particle detection, covered an angular region of  $\Delta\theta = 7.5^\circ$  and were centered at  $17.5^\circ$  and  $25.0^\circ$ , respectively. The other three PSDs were placed on the opposite side with respect to the beam axis, at the symmetrical angles. Two ionization chambers were used as  $\Delta E$  detectors to discriminate nitrogen from carbon ions, thus allowing the distinction between the  $^2\text{H}(^{17}\text{O},\alpha^{14}\text{N})n$  and  $^2\text{H}(^{17}\text{O},\alpha^{14}\text{C})p$  channels. The selection of the  $^2\text{H}(^{17}\text{O},\alpha^{14}\text{N}_{g.s.})n$  channel is accomplished following the standard procedure in Refs. [25,26]. No additional processes show up, because a single peak is present in the experimental  $Q$ -value spectrum (Fig. 1), centered at the theoretical value ( $Q = -1.033$  MeV).

Compelling evidence for the occurrence of the QF mechanism is given by the shape of the measured neutron momentum distribution: an observable very sensitive to the reaction mechanism. The experimental momentum distribution for the  $p$ - $n$  intercluster motion extracted from the present experiment was derived by following the standard procedure described in Ref. [29]. The experimental data, with their statistical error, are shown in Fig. 2 as a black points, and they are compared with the square of the Hulthén function in momentum space (black line in Fig. 2), representing the shape of the  $n$ - $p$  momentum distribution inside the deuteron in the plane-wave impulse

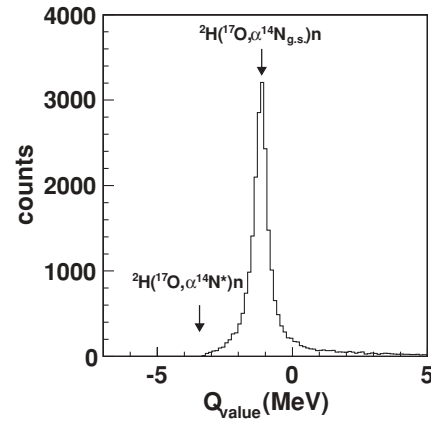


FIG. 1. Experimental  $Q$ -value spectrum. A single peak shows up, centered at about  $-1.0$  MeV, corresponding to the  $^{17}\text{O} + ^2\text{H} \rightarrow \alpha + ^{14}\text{N}_{g.s.} + n$  channel. The expected position of the  $^{17}\text{O} + ^2\text{H} \rightarrow \alpha + ^{14}\text{N}^* + n$  peak is also marked. Its occurrence is ruled out with high confidence, as the contribution of higher excited states.

approximation (PWIA):

$$\Phi(p_s) = \frac{1}{\pi} \sqrt{\frac{ab(a+b)}{(a-b)^2}} \left[ \frac{1}{a^2 + p_s^2} - \frac{1}{b^2 + p_s^2} \right], \quad (1)$$

with parameters  $a = 0.2317 \text{ fm}^{-1}$  and  $b = 1.202 \text{ fm}^{-1}$  [30] for the deuteron. To check if the simple PWIA approach gives an accurate description of the  $n$ - $p$  momentum distribution, the data were also compared with the DWBA distribution (red dotted line in Fig. 2), which is evaluated by means of the FRESKO code [31]. In the calculation, optical potential parameters adjusted from the Perey and Perey compilation [32] were adopted. From the comparison, we can state that a good agreement between DWBA and PWIA is present, within the experimental uncertainties, for a neutron momentum  $|p_s| < 30 \text{ MeV}/c$ . This demonstrates that the PWIA approach constitutes a viable approach to extract the resonance parameters

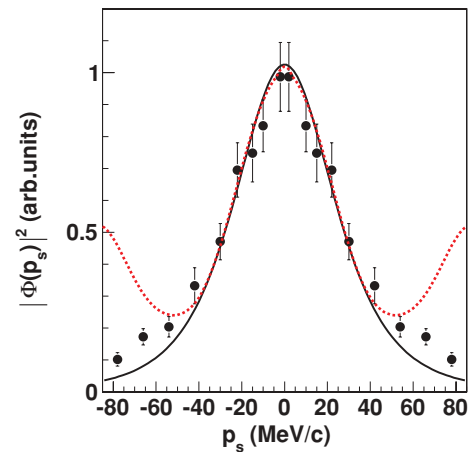


FIG. 2. (Color online) Experimental momentum distribution (full dots) compared with the theoretical ones, given by the square of the Hulthén function (black solid line) in the PWIA and by the distorted-wave Born approximation (DWBA) momentum distribution evaluated using the FRESKO code (red dotted line).

for the  $^{17}\text{O}(p,\alpha)^{14}\text{N}$  reaction as long as  $|p_s| < 30 \text{ MeV}/c$ . The good agreement between the experimental data and the theoretical calculations proves that in the selected kinematical region, the QF mechanism gives the main contribution to the  $^2\text{H} + ^{17}\text{O}$  interaction and that it can be selected without significant interference from contaminant sequential decay processes.

For these reasons, the further data analysis was performed by considering coincidence events with a neutron momentum ranging between  $-30$  and  $30 \text{ MeV}/c$ , allowing us to apply the PWIA in the following calculations.

As described in detail in Refs. [33,34], the  $2 \rightarrow 3$  reaction  $a + A \rightarrow s + c + C$  can be regarded as a two-step process, namely, the stripping  $a + A \rightarrow s + F$  to a resonant state in the compound system  $F$ , which later decays to the  $c + C$  channel. Correspondingly, the cross section of such a  $2 \rightarrow 3$  process can be factorized and the resonance parameters can be deduced from the experimental TH data. In particular, the TH double differential cross section of the  $^2\text{H}(^{17}\text{O}, ^{14}\text{N})n$  reaction can be written as [33–36]

$$\frac{d^2\sigma^{\text{TH}}}{d\Omega_n dE_{c.m.}} = \frac{1}{2\pi} \frac{\Gamma_{\alpha^{14}\text{N}}(E_{c.m.})}{(E_{c.m.} - E_{R_i})^2 + \frac{1}{4}\Gamma_i^2(E_{c.m.})} \frac{d\sigma_{[d(^{17}\text{O}, ^{18}\text{F}_i)n]}}{d\Omega_n}, \quad (2)$$

where  $\frac{d\sigma_{[d(^{17}\text{O}, ^{18}\text{F}_i)n]}}{d\Omega_n}$  is the differential cross section for the transfer  $^{17}\text{O} + d \rightarrow ^{18}\text{F}_i + n$  populating the  $i$ th resonant state in  $^{18}\text{F}$  with resonance energy  $E_{R_i}$ ,  $\Gamma_{\alpha^{14}\text{N}}(E_{c.m.})$  is the partial resonance width for the decay  $^{18}\text{F}_i \rightarrow \alpha + ^{14}\text{N}$ , and  $\Gamma_i$  is the total resonance width of the  $i$ th level in the  $^{18}\text{F}$  compound nucleus (see Ref. [34] and reference therein). The variable  $E_{c.m.}$  is the  $^{17}\text{O}-p$  relative kinetic energy related to the  $\alpha-^{14}\text{N}$  relative energy,  $E_{\alpha^{14}\text{N}}$ , by the energy conservation law,  $E_{c.m.} = E_{\alpha^{14}\text{N}} - Q_2$ , where  $Q_2 = 1.192 \text{ MeV}$  is the  $Q$  value of the  $^{17}\text{O}(p,\alpha)^{14}\text{N}$  reaction (see, e.g., Ref. [24] and references therein). These recent theoretical results demonstrate that the binary reaction cross section is not affected by the Coulomb barrier penetration effect, strongly confirming the main feature of the THM. In fact, in Eq. (2), the partial resonance width in the entrance channel  $\Gamma_{(p^{17}\text{O})}$ , does not appear; thus, it is possible to extend the measurement down to zero  $E_{c.m.}$  energy.

The resulting  $^{17}\text{O}(p,\alpha)^{14}\text{N}$  reaction cross section, integrated over the whole  $\theta_{c.m.}$  angular range, is shown in Fig. 3 (full circles). Horizontal error bars represent the integration energy bin, while the solid line represents the fit of the two-body cross section using three Gaussian functions to describe the resonant behavior and a straight line to account for the nonresonant contribution to the cross section. No interference effect is taken into account, since the natural widths of the resonances ( $\sim \text{eV}$ ) are much smaller than their energy separation ( $\sim \text{keV}$ ).

Because of the energy resolution ( $\sim 20 \text{ keV}$ ), the resonance at  $65 \text{ keV}$  was not well separated from the high-energy tail of the  $-3 \text{ keV}$  subthreshold state, corresponding to the  $E_X = 5.603 \text{ MeV}$  state of  $^{18}\text{F}$ . The subthreshold as well as the nonresonant contributions were evaluated so that the experimental TH angular distributions for the  $183 \text{ keV}$  resonance were in agreement with the experimental ones [13] and with the theoretical prediction for both the  $65$  and  $183 \text{ keV}$

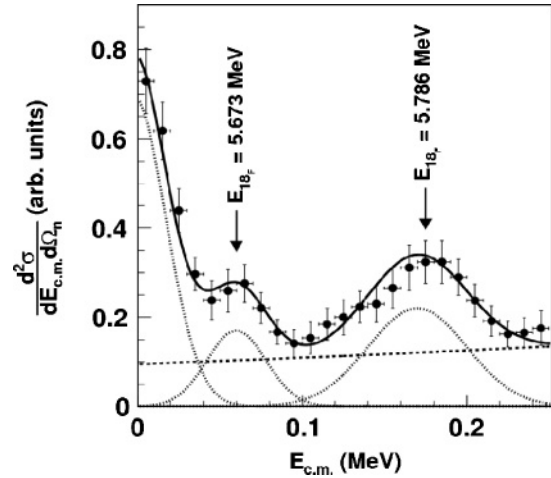


FIG. 3. Cross section of the TH reaction (full circles). The full line represents the result of a fit including three Gaussian curves and a first-order polynomial to take into account the nonresonant contribution to the cross section.

resonances based on the general theory reported in Ref. [37]. More details about such procedure will be presented in a subsequent extensive paper.

The fit was performed to extract the resonance energies:  $E_{R_1} = 60 \pm 5 \text{ keV}$  and  $E_{R_2} = 175 \pm 5 \text{ keV}$  (in fair agreement with the ones given in the literature [13]) and to deduce the peak values of the two resonances with their statistical errors:  $N_1 = 0.1700 \pm 0.0250_{\text{stat}}$  and  $N_2 = 0.2200 = \pm 0.0310_{\text{stat}}$ . Moreover, the  $N_1$  and  $N_2$  values are also affected by the uncertainty due to the nonresonant background estimation as well as by the uncertainty due to the peak-value correlation in the fit. For that reason, a detailed investigation into these sources of uncertainties was also performed. In particular, the nonresonant contribution was evaluated by means of the first-order polynomial,  $f(E_{c.m.}) = a_1 + a_2 E_{c.m.}$ , where  $a_1$  and  $a_2$  are fitting parameters. The simple linear parametrization of the background is well suited, since the energy range covered in the center-of-mass system is very narrow ( $250 \text{ keV}$ ), so no dramatic change in the nonresonant contribution is expected [34]. To evaluate the uncertainty due to the nonresonant background contribution, the central, lower, and upper values of  $a_1$  and  $a_2$  allowed by the fit were taken into account in both  $N_1$  and  $N_2$  calculations. Regarding the uncertainty due to the correlation between the  $N_1$  and  $N_2$  values in the fit, the maximum (minimum) value of  $N_1$  was evaluated fixing the minimum (maximum) value of  $N_2$  allowed by the fit. The same procedure was adopted for  $N_2$ . The described procedures lead to  $N_1 = 0.1700 \pm 0.0250_{\text{stat}} \pm 0.0040_{\text{back}} \pm 0.0003_{\text{corr}}$  and  $N_2 = 0.2200 \pm 0.0310_{\text{stat}} \pm 0.0060_{\text{back}} \pm 0.0002_{\text{corr}}$  (standard deviation), respectively. The obtained peak values, defined in Refs. [33,34] by using the plane-wave approximation, were then used to derive the resonance strengths:

$$(\omega\gamma)_i = \frac{2J_{^{18}\text{F}_i} + 1}{(2J_{^{17}\text{O}} + 1)(2J_p + 1)} \frac{\Gamma_{(p^{17}\text{O})_i}(E_{R_i})\Gamma_{(\alpha^{14}\text{N})_i}(E_{R_i})}{\Gamma_i(E_{R_i})}, \quad (3)$$

which are the relevant parameters for astrophysical application in the case of narrow resonances [38]. In this work, we did not measure the absolute value of the cross section; therefore, the absolute strength of the resonance at 65 keV was obtained from the ratio between the  $N_1$  and  $N_2$  peak values through the relation [34]

$$(\omega\gamma)_1 = \frac{\omega_1 \Gamma_{(p^{17}\text{O})_1} \sigma_{R_2}(\theta) N_1}{\omega_2 \sigma_{R_1}(\theta) \Gamma_{(p^{17}\text{O})_2} N_2} (\omega\gamma)_2, \quad (4)$$

where the subscripts 1 and 2 refer to the 65 and 183 keV resonances, respectively,  $\omega_i = (2J_{i8\text{F}_i} + 1)/[(2J_{17\text{O}} + 1)(2J_p + 1)]$  ( $i = 1, 2$ ) is the statistical factor,  $\sigma_{R_i}(\theta)$  is the direct transfer reaction cross section for the binary reaction  $A + a \rightarrow F_i + s$  populating the resonant state  $F_i$  with resonance energy  $E_{R_i}$  and  $\Gamma_{(p^{17}\text{O})_i}$  is the partial width for the  $p + {}^{17}\text{O} \rightarrow {}^{18}\text{F}_i$  channel, leading to the population of the  $i$ th excited state in  ${}^{18}\text{F}$  [34].

By taking  $(\omega\gamma)_2 = (1.66 \pm 0.10) \times 10^{-3}$  eV, namely, the weighted average of the three values for the 183 keV resonance strength given in the literature [13–15], by means of Eq. (4) one gets

$$(\omega\gamma)_1 = (3.66_{-0.64}^{+0.76}) \times 10^{-9} \text{ eV}. \quad (5)$$

When determining  $(\omega\gamma)_1^{\text{THM}}$ , the effect of energy resolution in our experiment was taken into account. Regarding the model uncertainty, this is less than about 10% because of the absence of any spectroscopic factor and the use of a double ratio compensating for the errors due to, for instance, the choice of the interaction radius [34]. Considering the upper and lower limits, the resulting  $(\omega\gamma)_1^{\text{THM}}$  value is in agreement with the value of  $(\omega\gamma)_N = (5.5_{-1.5}^{+1.8}) \times 10^{-9}$  eV adopted in NACRE, obtained by using the partial widths  $\Gamma_\alpha = 130$  eV [39] and  $\Gamma_p = 22 \pm 3$  neV [10] and with the  $(\omega\gamma)_D = (4.7 \pm 0.8) \times 10^{-9}$  eV value calculated by using  $\Gamma_\alpha = 130$  eV [39] and  $\Gamma_p = 19 \pm 3$  neV [12,40].

The resulting TH strength of the 65 keV resonance was used to calculate its contribution to the total reaction rate, and it was compared with the rate given by NACRE [38] and in Ref. [13]. To calculate the  ${}^{17}\text{O}(p,\alpha){}^{14}\text{N}$  reaction rate, we adopted the narrow resonance approximation, whose conditions are satisfied for the resonance under investigation. According to this approximation, the contribution of the 65 keV resonance to the rate  $R$  is given by

$$N_A \langle \sigma v \rangle_{R_1} = N_A \left( \frac{2\pi}{\mu k_B} \right)^{3/2} \hbar^2 (\omega\gamma)_1 T^{-3/2} \exp\left(-\frac{E_{R_1}}{k_B T}\right), \quad (6)$$

where  $\mu$  is the reduced mass for the projectile-target system,  $k_B$  is the Boltzmann constant, and  $T$  is the temperature of the astrophysical site. In the upper part of Fig. 4, the ratio of the THM reaction rate to the NACRE one for the  ${}^{17}\text{O}(p,\alpha){}^{14}\text{N}$  reaction is shown as a full black line, while the NACRE rate is given by a full red line. The dot-dashed and dotted lines represent the 65 keV upper and lower limits, respectively, allowed by the experimental uncertainties. In the lower part of Fig. 4, the ratio of the THM reaction rate to that obtained in Ref. [13] is shown and, as before, black and red lines mark THM and Chafa rate, respectively. Also in this case,

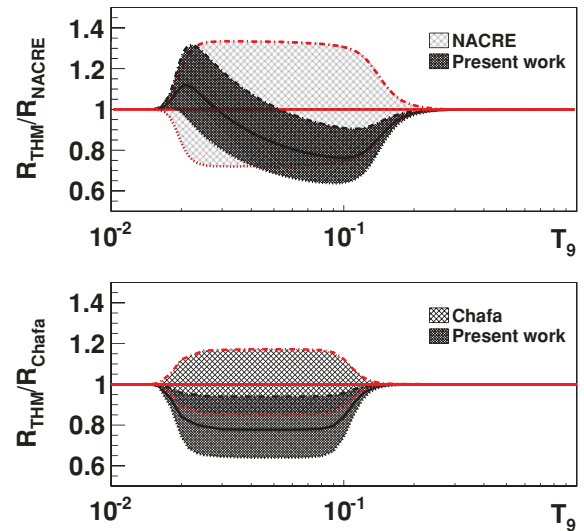


FIG. 4. (Color online) Comparison of the reaction rate of the  ${}^{17}\text{O}(p,\alpha){}^{14}\text{N}$  reaction with the NACRE reaction rate [38] (upper panel) and Chafa one [13] (lower panel). More details in the text.

the experimental uncertainties due to the 65 keV resonance only are shown as dot-dashed and dotted lines, respectively.

Figure 4 shows that in the low-temperature region (below  $T_9 = 0.2$ ) the value of the extracted  ${}^{17}\text{O}(p,\alpha){}^{14}\text{N}$  reaction rate is about 20% smaller than that given in Ref. [13], which is the most recent and accurate reaction rate determination in the literature so far.

Although the 20% difference between the two measurements is within the quoted experimental uncertainties, a possible explanation of such discrepancy could be due to the electron screening effect that was not taken into account in the direct measurement [10]. The problem of the electron screening has been addressed for a nonresonant reaction [41] or for a reaction showing broad resonances [42–44]. When a reaction cross section is dominated by narrow resonances, as in the present case, the electron screening correction depends on the relative magnitude of the incoming and outgoing partial widths, and its theoretical treatment is more complicated than in the previous cases [42]. Such treatment is extensively studied in Refs. [43,44], where an explicit expression for the enhancement factor is deduced for stellar plasma. Anyway, their conclusion can be easily extended to the electron screening enhancement in the laboratory. In a naive picture, a very simple relationship between the screened and bare resonance strengths can be deduced. Since  $\omega\gamma$  is proportional to the proton partial width  $\Gamma_p = 2\gamma^2 P_l$ , where  $l = 1$  for the 65 keV resonance in the  ${}^{17}\text{O}(p,\alpha){}^{14}\text{N}$  cross section, by assuming that the penetration of the Coulomb barrier is taking place at a higher energy  $E + U_e$  due to the electron screening ( $U_e$  being the electron screening potential [16,41,45]), we obtain

$$(\omega\gamma)_{\text{screen}}/(\omega\gamma)_{\text{bare}} \sim \exp(\pi\eta U_e/E) = f_{\text{lab}}(E). \quad (7)$$

Therefore, in a first approximation, the usual enhancement factor can be recovered.

To verify that the electron screening effect might be a valid explanation for the 20% discrepancy between direct and THM

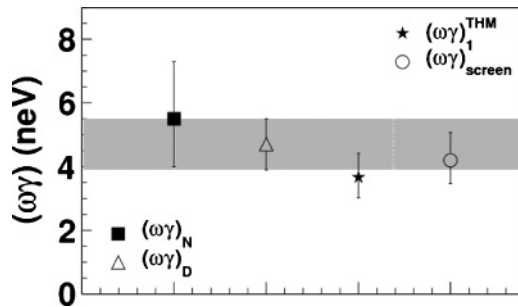


FIG. 5. Comparison between the different values of the 65 keV resonance strength discussed in the text. The gray band represents the recommended range deduced in Ref. [13].

data, the indirect 65 keV resonance strength [Eq. (5)] was multiplied by the value of the enhancement factor  $f_{\text{lab}} = 1.148$  from Ref. [16], obtaining the resonance strength  $(\omega\gamma)_{\text{screen}}$ , which accounts for the electron screening effect,

$$(\omega\gamma)_{\text{screen}} = f_{\text{lab}}(\omega\gamma)_1^{\text{THM}} = (4.21^{+0.87}_{-0.73}) \times 10^{-9} \text{ eV}. \quad (8)$$

This value represents just the lower limit for the screened strength, since the electron screening potential turns out to be much larger than the theoretical upper limit in most

cases [41,45]. Though error bars are large,  $(\omega\gamma)_{\text{screen}}$  is clearly in better agreement with the  $(\omega\gamma)_D$ , as demonstrated in Fig. 5. Indeed, if just the electron screening enhancement is taken into account, the central value of the THM strength lies within the recommended range from Ref. [13].

To make the comparison more quantitative,  $\bar{\chi}^2$  was evaluated for  $(\omega\gamma)_1^{\text{THM}}$  and  $(\omega\gamma)_{\text{screen}}$ . In the former case,  $\bar{\chi}^2 = 1.7$  was obtained, while, if screening is taken into account,  $\bar{\chi}^2 = 0.4$ . This test demonstrates that a viable reason for the difference is the electron screening. This difference can in no way be neglected in astrophysical applications, because stellar observables are very sensitive to the  $^{17}\text{O}(p,\alpha)^{14}\text{N}$  strength. The advantage of the THM approach is that the strength is free of the most common sources of systematic uncertainties affecting low-energy direct measurements.

The astrophysical implications of our results will be the subject of a forthcoming dedicated paper.

The work was supported in part by the US Department of Energy under Grant No. DE-FG02-93ER40773 and DE-FG52-06NA26207, NSF under Grant No. PHY-0852653 and by the Italian Ministry of University and Research under Grant No. RBFR082838 (FIRB2008).

- 
- [1] M. Hernanz *et al.*, *Astrophys. J.* **526**, L97 (1999).  
 [2] J. José and M. Hernanz, *J. Phys. G* **34**, R431 (2007).  
 [3] K. M. Nollett *et al.*, *Astrophys. J.* **582**, 1036 (2003).  
 [4] A. I. Boothroyd *et al.*, *Astrophys. J.* **442**, L21 (1995).  
 [5] S. Palmerini *et al.*, *Pub. Astron. Soc. Aust.* **26**, 161 (2009).  
 [6] R. E. Brown, *Phys. Rev.* **125**, 347 (1962).  
 [7] C. Rolfs and W. S. Rodney, *Nucl. Phys. A* **250**, 295 (1975).  
 [8] W. E. Kieser *et al.*, *Nucl. Phys. A* **331**, 155 (1979).  
 [9] V. Landre *et al.*, *Phys. Rev. C* **40**, 1972 (1989).  
 [10] J. C. Blackmon *et al.*, *Phys. Rev. Lett.* **74**, 2642 (1995).  
 [11] C. Fox *et al.*, *Phys. Rev. Lett.* **93**, 081102 (2004).  
 [12] C. Fox *et al.*, *Phys. Rev. C* **71**, 055801 (2005).  
 [13] A. Chafa *et al.*, *Phys. Rev. C* **75**, 035810 (2007).  
 [14] B. H. Moazen *et al.*, *Phys. Rev. C* **75**, 065801 (2007).  
 [15] J. R. Newton, C. Iliadis, A. E. Champagne, R. Longland, and C. Ugalde, *Phys. Rev. C* **75**, 055808 (2007).  
 [16] H. J. Assenbaum *et al.*, *Z. Phys. A* **327**, 461 (1987).  
 [17] G. Baur *et al.*, *Phys. Lett. B* **178**, 135 (1986).  
 [18] S. Cherubini *et al.*, *Astrophys. J.* **457**, 855 (1996).  
 [19] C. Spitaleri *et al.*, *Phys. Rev. C* **60**, 055802 (1999).  
 [20] G. Calvi *et al.*, *Nucl. Phys. A* **621**, 139 (1997).  
 [21] M. Lattuada *et al.*, *Astrophys. J.* **562**, 1076 (2001).  
 [22] C. Spitaleri *et al.*, *Phys. Rev. C* **63**, 055801 (2001).  
 [23] A. Tumino *et al.*, *Phys. Rev. C* **67**, 065803 (2003).  
 [24] C. Spitaleri *et al.*, *Phys. Rev. C* **69**, 055806 (2004).  
 [25] M. La Cognata *et al.*, *Phys. Rev. C* **72**, 065802 (2005).  
 [26] A. Tumino *et al.*, *Eur. Phys. J. A* **27**, 243 (2006).  
 [27] M. La Cognata *et al.*, *Phys. Rev. C* **76**, 065804 (2007).  
 [28] A. Tumino *et al.*, *Phys. Rev. Lett.* **98**, 252502 (2007).  
 [29] R. G. Pizzone *et al.*, *Phys. Rev. C* **80**, 025807 (2009).  
 [30] M. Zadro *et al.*, *Phys. Rev. C* **40**, 181 (1989).  
 [31] I. J. Thompson, *Comput. Phys. Rep.* **7**, 167 (1987).  
 [32] C. M. Perey and F. G. Perey, *At. Data Nucl. Data Tables* **17**, 1 (1976).  
 [33] M. La Cognata *et al.*, *Phys. Rev. Lett.* **101**, 152501 (2008).  
 [34] M. La Cognata *et al.*, *Astrophys. J.* **708**, 796 (2010).  
 [35] E. I. Dolinsky *et al.*, *Nucl. Phys. A* **202**, 97 (1973).  
 [36] A. M. Mukhamedzhanov *et al.*, *J. Phys. G* **35**, 014016 (2008).  
 [37] J. M. Blatt and L. C. Biedenharn, *Rev. Mod. Phys.* **24**, 258 (1952).  
 [38] C. Angulo *et al.*, *Nucl. Phys. A* **656**, 3 (1999).  
 [39] H. B. Mak *et al.*, *Nucl. Phys. A* **343**, 79 (1980).  
 [40] M. D. Hannam and W. J. Thompson, *Nucl. Instrum. Methods A* **431**, 239 (1999).  
 [41] F. Strieder *et al.*, *Naturwissenschaften* **88**, 461 (2001).  
 [42] C. Iliadis, *Nuclear Physics of Star* (Wiley-VCH Verlag GmbH & Co. KGaA, New York, 2007).  
 [43] E. E. Salpeter and H. M. Van Horn, *Astrophys. J.* **155**, 183 (1969).  
 [44] H. E. Mittleer, *Astrophys. J.* **212**, 513 (1977).  
 [45] G. Fiorentini *et al.*, *Z. Phys.* **350**, 289 (1995).